

<https://it.overleaf.com/project/6547d57852b0d7a8ee70cf67>

## The MEG II experiment: status and perspectives

---

**Antoine Venturini<sup>a,b,\*</sup> on behalf of the MEG II Collaboration**

<sup>a</sup>*Università di Pisa, Dipartimento di Fisica,  
Largo B. Pontecorvo 3, 56127 Pisa, Italy*

<sup>b</sup>*INFN Sezione di Pisa,  
Largo B. Pontecorvo 3, 56127 Pisa, Italy*

*E-mail: [antoine.venturini@pi.infn.it](mailto:antoine.venturini@pi.infn.it)*

We report about the status of the MEG II experiment and its physics program. The MEG II experiment has been constructed to search for the charged lepton flavor violating process  $\mu^+ \rightarrow e^+\gamma$ . Physics data taking started in 2021 and is planned to continue until 2026. We report the result of the analysis of the 2021 dataset, which yield no evidence of the  $\mu^+ \rightarrow e^+\gamma$  decays. We summarize as well the status of the experimental activities ongoing on other two topics: the search for the  $X(17)$  boson and for the charged lepton flavor violating process  $\mu^+ \rightarrow e^+a\gamma$ , with  $a$  being an hypothetical axion-like particle.

*Workshop Italiano sulla Fisica ad Alta Intensità (WIFAI2023)  
8-10 November 2023*

*Dipartimento di Architettura dell'Università Roma Tre, Rome, Italy*

---

\*Speaker

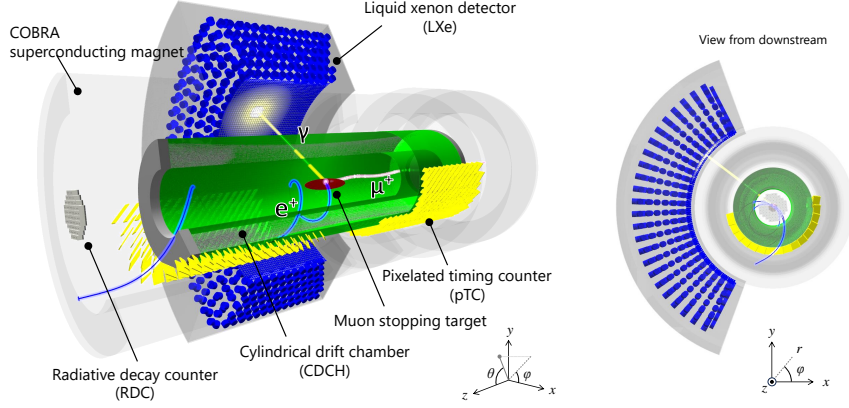


**Figure 1:** MEG II detector scheme with a simulated  $\mu^+ \rightarrow e^+\gamma$  event [4].

## 1. Introduction

Within the Standard Model (SM) of Particle Physics incorporating massive neutrinos, charged lepton flavor-violating (cLFV) processes are notably suppressed. An example of such processes is the  $\mu \rightarrow e\gamma$  decay, characterized by expected branching ratios at the scale of  $O(10^{-50})$ . Due to these negligible expected values within the SM, any experimental detection of excesses in cLFV processes would be compelling evidence for the existence of New Physics beyond the SM. Predictions in most SM extensions suggest the potential for observable rates in cLFV processes, motivating new experimental efforts. A comprehensive overview of the theoretical and experimental landscape of cLFV searches is available in [1] and associated references.

The MEG II collaboration is searching for the  $\mu^+ \rightarrow e^+\gamma$  decay at the Paul Scherrer Institut (PSI) muon beam facility. Its goal is to refine the sensitivity of the branching ratio for this decay to  $\mathcal{B}(\mu^+ \rightarrow e^+\gamma) < 6 \times 10^{-14}$  (90% CL). This marks a significant improvement, achieving an order of magnitude greater precision compared to the current limit set by the MEG experiment, which holds the best limit at  $\mathcal{B}(\mu^+ \rightarrow e^+\gamma) < 4.2 \times 10^{-13}$  (90% CL) [2]. This paper succinctly presents key aspects of the MEGII experiment and unveils its first results on the search for the  $\mu \rightarrow e\gamma$  decay using data from the year 2021. Additional details regarding this measurement can be accessed in [3].

## 2. The MEG II apparatus

The MEG II experiment is located downstream the  $\pi E5$  beam line at PSI delivering a continuous beam of positive muons with an average momentum of 28 MeV/c that can be stopped in a thin plastic target at the center of the apparatus. A signal from the  $\mu^+ \rightarrow e^+\gamma$  decay has a clear signature in the center-of-mass frame (in MEG II this coincides with the laboratory frame): a positron ( $e^+$ ) and a photon ( $\gamma$ ) are emitted at the same time ( $t_{e\gamma} \equiv t_e - t_\gamma = 0$ ) in opposite directions ( $\Theta_{e\gamma} \equiv$  angle between directions of flight =  $\pi$ ) and with almost the same energy ( $E_{e^+} \approx E_\gamma \approx m_\mu c^2/2 \approx 52.83$  MeV). MEG II's detector system, which mainly consists of a magnetic spectrometer and a photon detector (Figure 1), has been optimized to improve the resolutions for  $e^+$  and  $\gamma$  measurements, which

**Table 1:** Detectors' resolutions and efficiencies at  $3 \times 10^7 \mu^+ \text{s}^{-1}$  beam intensity. Derived from [4].

Resolutions				Efficiencies		
$\sigma_{E_\gamma}$	$\sigma_{p_e}$	$\sigma_{t_{e\gamma}}$	$\sigma_{\Theta_{e\gamma}}$	$\epsilon_{e^+}$	$\epsilon_\gamma$	$\epsilon_{Trigger}$
1.8-2.0% @ 52.83 MeV	89 keV	78 ps	14.1 rad	67%	62%	80%

is crucial to distinguish a signal event from background ones. The experimental background consists of two phenomena [5]: radiative muon decays (RMD)  $\mu^+ \rightarrow e^+\gamma\nu\bar{\nu}$  and accidental coincidences (the dominant background) between high energy  $e^+$  and  $\gamma$ . Detectors are constructed to achieve optimal performances in an extremely radiation-cluttered environment. A high muon rate is indeed essential to have large statistics (the rate of the continuous muon beam was varied during 2021 data-taking between 2 and  $5 \times 10^7 \mu^+ \text{s}^{-1}$ ). More details about MEG II apparatus (including calibrations) can be found in [4], while performances measured on 2021 data are listed in Table 1.

The magnetic spectrometer consists of three parts: a spatially-varying magnetic field created by the COBRA (Constant Banding Radius) superconducting magnet in which positrons curve; a single volume, ultra-low cylindrical drift chamber with 1728 signal wires [6] that tracks the positrons trajectories; a pixelated Timing Counter detector [7] (pTC), comprising 512 scintillating tiles readout by SiPMs, which provides precise positron timing and prompt information about their trajectory, both used at the trigger level.

The  $\gamma$  detector employs 900 liters of liquid xenon as a scintillating material (high purity, high light yield, fast scintillation). The scintillation light is readout by 4092 SiPMs [8] on the entrance face of the detector for good position resolution of the interaction vertex. The sides and back of the detector volume are instrumented with 668 PMTs.

The MEG II experiment also benefits of an auxiliary detector (the Radiative Decay Counter, RDC), composed of scintillating bars and a LYSO calorimeter, to tag low energy positrons which may coincide with energetic photons: this helps in identifying RMD decays which, in coincidence with an energetic  $e^+$ , can contribute to the accidental background, thereby reducing the background contamination.

The trigger and data-acquisition form an integrated system in MEG II [9, 10]: a sophisticated trigger employing on FPGAs selects candidate signal events based on online estimates of  $t_{e^+\gamma}$ ,  $E_\gamma$  and  $\Theta_{e^+\gamma}$ ; for each triggered event, the waveform of each detector channel (more than 9000) is digitized for precise offline reconstruction.

### 3. Data analysis with the 2021 dataset

The confidence interval on the number of  $\mu^+ \rightarrow e^+\gamma$  signal events  $N_{sig}$  is determined through an unbinned maximum likelihood fit of the data. Confidence intervals for  $N_{sig}$  are built following the Feldman-Cousins prescription using the profile likelihood ratio ordering [11]. The likelihood  $\mathcal{L}$  is a function of the following observables  $\vec{x}_i = \{E_\gamma, E_{e^+}, t_{e^+\gamma}, \Theta_{e^+\gamma}$  (or  $\theta_{e^+\gamma}, \phi_{e^+\gamma}$ , which are the azimuthal and polar projection of  $\Theta_{e^+\gamma}$ , as defined in [3]),  $t_{RDC} - t_{LXe}$ ,  $E_{RDC}$ ,  $n_{pTC}\}$  (the number of hits in the pTC). The likelihood function is parameterized also by three *nuisance parameters* which are additional degrees of freedom (the total number of fit parameters is four): the number of

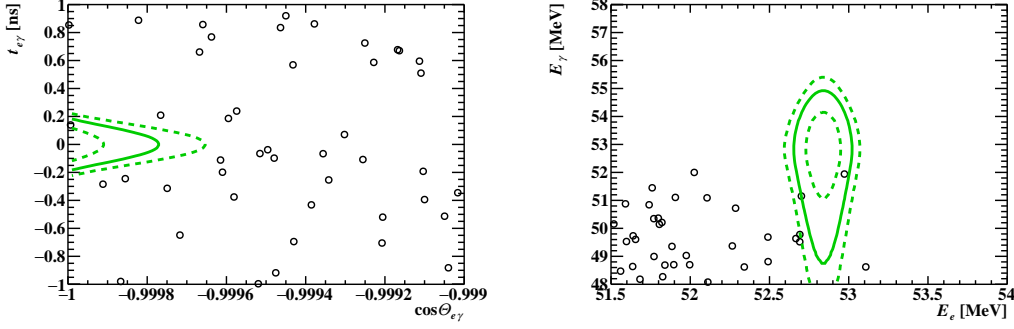


**Figure 2:** Distributions of events inside (part of) the signal region: left)  $\cos \Theta_{e^+\gamma} - t_{e^+\gamma}$  plane; right)  $E_{e^+} - E_{\gamma}$  plane. Signal PDFs contours (for 1, 1.64, 2  $\sigma$ ) are drawn with green lines.

background events  $N_{RMD}$  and  $N_{ACC}$  and the target position  $x_T$ . The extended likelihood function is:

$$\mathcal{L}(N_{sig}, N_{RMD}, N_{ACC}, x_T) = \frac{e^{-(N_{sig}+N_{RMD}+N_{ACC})}}{N_{obs}!} C(N_{RMD}, N_{ACC}, x_T) \times \prod_{i=1}^{N_{obs}} (N_{sig} Sig(\vec{x}_i) + N_{RMD} RMD(\vec{x}_i) + N_{ACC} ACC(\vec{x}_i))$$

where  $C$  is the product of the gaussian constraints on the nuisance parameters and  $Sig$ ,  $RMD$ ,  $ACC$  are the probability density functions (PDFs) of the signal and the background respectively. Initial values for the nuisance parameters are determined and the PDFs for signal and background are built analyzing data (also using Monte Carlo simulations) outside a "blinding box": data satisfying the conditions  $48.0 < E_{\gamma} < 58.0$  MeV and  $|t_{e^+\gamma}| < 1$  ns are hidden and can't be used for calibration in order to avoid any bias in the final analysis.

From the fitted value of  $N_{sig}$ , the branching ratio of  $\mu^+ \rightarrow e^+\gamma$  is derived using  $B = N_{sig}/N_{\mu}$ ,  $N_{\mu}$  being the total number of muons observed to decay in the experiment. For the 2021 data-taking,  $N_{\mu}$  has been measured to be  $N_{\mu} = (2.64 \pm 0.12) \times 10^{12}$ . The MEG II sensitivity @90% C. L.  $\mathcal{S}_{90}^1$  for 2021 is  $\mathcal{S}_{90} = 8.1 \times 10^{-13}$ , which is already close to the MEG final sensitivity, although the total number of stopped muons is much lower: this is due to the detectors' upgraded performances and efficiencies.

After unblinding of 2021 data, the likelihood fit was performed and yielded no evidence for the  $\mu^+ \rightarrow e^+\gamma$  decay: the 90% CL upper limit of the branching ratio is

$$\mathcal{B}(\mu^+ \rightarrow e^+\gamma) < 7.5 \times 10^{-13} \text{ (90\% C. L.)}$$

In Figure 2 we show the event distribution inside the analysis region. No event falls inside the 2 -  $\sigma$  signal region.

A more stringent upper limit is determined combining these results with MEG ones using the product of the likelihood functions from the two experiments. The combined branching ratio is

$$\mathcal{B}(\mu^+ \rightarrow e^+\gamma) = 3.1 \times 10^{-13} \text{ (90\% C. L.)}$$

<sup>1</sup> $\mathcal{S}_{90} \equiv$  median of the distribution of 90% C. L. upper limit from 1000 pseudo-experiments.

which is the most stringent limit up to date.

#### 4. Beyond $\mu^+ \rightarrow e^+\gamma$ @MEG II

**The search for the X(17) Boson** In 2016, at ATOMKI Laboratories in Hungary a new resonance was observed in the energy end angular distribution of  $e^+ - e^-$  pairs from the  ${}^7\text{Li}(p, e^+e^-){}^8\text{Be}$  process [12]. Such a resonance is compatible with the hypothesis of a new boson with mass  $m \approx 17 \text{ MeV}/c^2$  (named X(17)) [13].

The MEG II Collaboration is in the position to validate these results independently [14]. Protons are accelerated up to 1080 keV with a Cockroft-Walton machine and impinge on a  $2 \mu\text{m}$  LiPON thin target placed at the center of the detector apparatus. The  $e^+ - e^-$  pairs produced in the  ${}^7\text{Li}(p, e^+e^-){}^8\text{Be}$  reaction are then tracked inside the MEG II spectrometer. So far, two data-taking campaigns have been conducted: an engineering run in 2022 and a physics data-taking in 2023, with  $E_p = 440 \text{ keV}$ . A second physics run is scheduled for 2024, while data collected in 2022 are being analyzed with the same strategy used for MEG II.

**The search for  $\mu^+ \rightarrow e^+a\gamma$  decays** Axion-like particles (ALP) are pseudo-scalar particles hypothesized in many models of New Physics, which may solve numerous puzzles of the SM. The existence of an ALP coupling to the SM fermions can induce cLFV processes, such as the  $\mu \rightarrow ea$  or  $\mu \rightarrow e a \gamma$  decay ( $a$  being the ALP) [15]. A phenomenological study [16] suggested that MEG II experiment is in position to search for the  $\mu^+ \rightarrow e^+a\gamma$  decay with better sensitivity than any other previous experiment. The interest in this decay channel motivated the MEG II collaboration to study the feasibility of this measurement [17]: preliminary results based on Monte Carlo simulations show that, exploiting data samples already collected in 2021 and 2022, new regions of the ALP-theory parameter space may be explorable with the current experimental sensitivity.

#### 5. Conclusions

The MEG II experiment started collecting data for the search of the cLFV decay  $\mu^+ \rightarrow e^+\gamma$  since 2021. The analysis of the first-year dataset has already answered two questions: first, it confirmed that the detector's performances match the project's ones, therefore the MEG II experiment is expecting to reach the goal sensitivity of  $S_{90}(\mu^+ \rightarrow e^+\gamma) = 6 \times 10^{-14}$  within 2026; second, having found no evidence for this decay, it allows to put new upper limit on the  $\mu^+ \rightarrow e^+\gamma$  decay when combining these results with the past best upper limit:  $\mathcal{B}(\mu^+ \rightarrow e^+\gamma) < 3.1 \times 10^{-13}$  (@ 90% C. L.).

In the upcoming years, the MEG II experiment is expected to contribute to searches also on other Physics channels. An experimental project to search for the X(17) boson started in 2022. The analysis of the 2023 data with  $E_p = 440 \text{ keV}$  is being completed and a second-year of physics data is scheduled in 2024. Again on the cLFV side, the abundance of  $\mu$  decays collected at various beam intensities allows also to explore other cLFV processes: studies are ongoing to evaluate the possibility for the MEG II Collaboration to search for the  $\mu^+ \rightarrow e^+a\gamma$  decay with an ALP in the final state.

## References

- [1] L. Calibbi, G. Signorelli, *Charged lepton flavour violation: an experimental and theoretical introduction*, *Riv. Nuovo Cim.* **41** (2018) 71.
- [2] A. M. Baldini et al., *Search for the lepton flavour violating decay  $\mu^+ \rightarrow e^+\gamma$  with the full dataset of the MEG experiment*, *Eur. Phys. J. C* **76** (2016) .
- [3] K. Afanaciev et al., *A search for  $\mu^+ \rightarrow e^+\gamma$  with the first dataset of the MEG II experiment*, [2310.12614](#).
- [4] K. Afanaciev et al., *Operation and performance of MEG II detector*, [2310.11902](#).
- [5] Y. Kuno, Y. Okada, *Muon decay and physics beyond the standard model*, *Rev. Mod. Phys.* **73** (2001) .
- [6] A. M. Baldini et al., *Performances of a new generation tracking detector: the MEG II cylindrical drift chamber*, [2310.12865](#).
- [7] M. Nishimura et al., *Full system of positron timing counter in MEG II having time resolution below 40 ps with fast plastic scintillator readout by siPMs*, *Nucl. Instrum. Methods A* **958** (2020) .
- [8] K. Ieki et al., *Large-area MPPC with enhanced VUV sensitivity for liquid xenon scintillation detector*, *Nucl. Instrum. Methods A* **925** (2019) .
- [9] L. Galli et al., *WaveDAQ: An highly integrated trigger and data acquisition system*, *Nucl. Instrum. Methods A* **936** (2019) .
- [10] M. Francesconi et al., *The waveDAQ integrated trigger and data acquisition system for the MEG II experiment*, *Nucl. Instrum. Methods A* **1045** (2023) .
- [11] G. J. Feldman, R. D. Cousins, *Unified approach to the classical statistical analysis of small signals*, *Phys. Rev. D* **57** (1998) .
- [12] A. J. Krasznahorkay et al., *Observation of anomalous internal pair creation in  $^8\text{Be}$ : A possible indication of a light, neutral boson*, *Phys. Rev. Lett.* **116** (2016) .
- [13] J. L. Feng et al., *Protophobic fifth-force interpretation of the observed anomaly in  $^8\text{Be}$  nuclear transitions*, *Phys. Rev. Lett.* **117** (2016) .
- [14] D. S. M. Alves et al., *Shedding light on X17: community report*, *Eur. Phys. J. C* **83** (2023) .
- [15] L. Calibbi et al., *Looking forward to lepton-flavor-violating alps*, *JHEP* **2021** (2021) .
- [16] Y. Jho, S. Knapen, D. Redigolo, *Lepton-flavor violating axions at MEG II*, *J. High Energy Phys.* **2022** (2022) .
- [17] E. G. Grandoni, *Studio di sensibilità del decadimento cLFV  $\mu \rightarrow e\alpha\gamma$  nell'esperimento MEG II*, Master's thesis, Università di Pisa, 2023.